

Optimisation of the Environmental Scanning Electron Microscope for Observation of Drying of Matt Water-Based Lacquers

C.P. ROYALL AND A.M. DONALD

Polymers and Colloids Group, Department of Physics, University of Cambridge, Cavendish Laboratory, Cambridge, U.K.

Summary: Environmental scanning electron microscopy (ESEM) modifies conventional SEM through the use of a partial gas pressure in the microscope specimen chamber. Like conventional SEM, it has the resolution to image structure on the submicron lengthscale, but can also tolerate hydrated specimens if water vapour is used in the specimen chamber. This ability to image aqueous specimens leaves ESEM uniquely placed to study in situ drying in polymer latexes. However, there are two key practical difficulties associated with in situ drying. First, the size of the latex particles: larger latex particles are typically around 500 nm in diameter. Although ESEM can resolve structure on this lengthscale without difficulty, the magnification required results in radiation damage of the specimen due to the electron beam. This means that a given region can be imaged only once during film formation, so the evolution of particular features cannot be followed. Second, the change from ambient temperature and pressure to the ESEM conditions of 7°C and 7.5 torr (100 Pa) can subject the specimen to a very high evaporation rate, which can disrupt film formation. The inclusion of a drop of water in the specimen chamber is shown largely to alleviate this, enabling successful imaging of film formation in the lacquer. Instead of the polymer latex itself, this work concentrates on a matting lacquer with silica inclusions. The silica matting agent particles are 1–10 µm in size, allowing for a lower magnification to be used, massively reducing specimen damage. Furthermore, the contrast during drying is much enhanced in the presence of silica. The images reveal the silica as bright regions against a darker background of polymer and water. Film formation shows the transition

from a uniform, featureless aqueous solution to a polymer film with silica particles present on the surface. The appearance of individual silica particles can be followed. The particles are generally revealed quite early, after a few minutes of drying time. As film formation progresses, these same particles appear larger and more distinct. Few new particles are revealed at longer film formation times.

Key words: environmental scanning electron microscope, latex, drying, hydrated

PACS: 68.37.-d, 68.37.Hk

Introduction

Polymer latexes, the basis of most water-based lacquers, have been studied extensively (Keddie 1997). Although the process of film formation is not yet fully understood, four stages have been proposed. The latex particles are initially dispersed in an aqueous medium (stage I) before being brought into a densely packed array (stage II) (Keddie 1997). Further evaporation is typically accompanied by deformation of the spherical polymer particles to form a continuous polymer film (stage III) (Brown 1956). Finally, the polymer undergoes interdiffusion in which the boundaries between the latex particles are broken down (stage IV) (Keddie 1997). The transition from stage II to III requires that the particles are sufficiently viscoelastic to deform before the water has evaporated. These latexes are termed film forming. Latexes with harder particles that do not deform prior to the evaporation of water are called non-film forming (Keddie *et al.* 1996). Keddie termed these arrays of undeformed latex particles stage II*. Here we focus on the stages of film formation associated with the removal of water, from stage I to III or II*.

The latex which forms the subject of this work has inclusions of precipitated silica. This has significant practical implications: the surface roughness imparted by the 1–10 µm aggregate particles is on the lengthscale of visible light, so specular reflection is much reduced (Gate *et al.* 1973). This combination of silica and latex is therefore used extensively as a matting lacquer (Schneider 1994).

Environmental scanning electron microscopy (ESEM) is well-suited to observing in situ drying of the matt lac-

C.P. Royall was supported by an EPSRC (Engineering and physical sciences research council) Studentship and a CASE award from Crosfield Group.

Address for reprints:

Prof. A.M. Donald
Polymers and Colloids Group
Department of Physics
University of Cambridge
Cavendish Laboratory
Madingley Road
Cambridge CB3 0HE, U.K.

quers for two main reasons: (1) It has the resolution to image the silica particles which dominate the surface structure, and (2) unlike conventional high-vacuum scanning electron microscopy (SEM), it can tolerate insulating and even hydrated specimens, such as the aqueous dispersion studied here (Danilatos 1993). Careful control of experimental conditions allows in situ film formation to be followed (Keddie *et al.* 1996).

However, ESEM has two key limitations that have hampered previous attempts to follow drying: Specimen damage from the electron beam and specimen stabilisation. Due to their high interfacial area, latexes are especially susceptible to reactive species formed in water by the electron beam (Royall *et al.* 2001, Talmon 1987). Keddie *et al.* (1996) imaged relatively large latex particles of approximately 500 nm in diameter. Although ESEM is easily able to resolve this lengthscale, the magnification required was 4000 \times . The radiation damage resulting from this magnification prevented successive imaging of the same area.

Radiation damage is much alleviated with the inclusion of silica. The larger size (1–10 μm) of the silica particles requires a magnification of only 800 \times . Since beam damage scales approximately with the square of magnification (Royall *et al.* 2001), the fivefold reduction in magnification relative to earlier work (Keddie *et al.* 1996) results in a very considerable decrease in radiation damage. If we assume that the electron beam penetrates around 10 μm into the specimen (Royall *et al.* 2001), there is a dose of approximately 12 kGy absorbed per image in the irradiated region at 800 \times , compared with 310 kGy at 5000 \times . In fact, scanning over a wider area allows successive imaging of the same region, which can be followed in real time.

The second limitation results from the pumpdown process, where ambient air is replaced by the partial pressure of water vapour used when hydrated systems are imaged by ESEM. This process can cause significant specimen damage or at least alteration due to uncontrolled water evaporation and boiling. This limitation is equally applicable to the matt water-based lacquer examined here as to the pure latexes examined by previous workers. The pumpdown process has been examined by Cameron and Donald (1994), who suggested a means to minimise water evaporation. Here we explore how evaporation can be further reduced with the introduction of a water source in the specimen chamber. The effect of this additional water source is considered using the model of Cameron and Donald (1994).

The images obtained by ESEM reveal silica particles as bright regions in a more uniform polymer/water background. Computational analysis of these images provides a quantitative measure of the microstructure evolution during drying. This article first examines the ESEM pumpdown process, and how it may be optimised for polymer latexes. The optimised pumpdown is then applied to a matting water-based lacquer.

Environmental Scanning Electron Microscope Pumpdown

Here we review the methodology and key relevant results of Cameron and Donald (1994). The ESEM is distinguished from the conventional SEM by maintaining a partial pressure of gas in the specimen chamber. However, the electron optics must be maintained in a reasonably high vacuum to avoid scattering of the electron beam. This requires a pressure gradient to be set up, so that the specimen chamber has a pressure of 1–10 torr, whereas the electron optics column has a relatively high vacuum (Danilatos 1993). The pressure gradient is maintained through constant pumping and the use of pressure limiting apertures (PLAs) which limit the flow of gas along the pressure gradient (Fig.1).

The key to stabilising hydrated specimens is the saturated vapour pressure (SVP), which is plotted in Figure 2 as a function of temperature. When a hydrated specimen is held at the saturated vapour pressure, the rates of evaporation and condensation are equal, so the specimen is stable. Increasing the temperature (holding the pressure constant) results in a net evaporation; conversely, decreasing the temperature causes a net condensation. The ESEM works best in the pressure range between 1–10 torr of water vapour, so to maintain equilibrium, the specimen must be chilled to a temperature of a few degrees Celsius. This chilling is accomplished with a specimen stage controlled with a Peltier chip (Danilatos 1993).

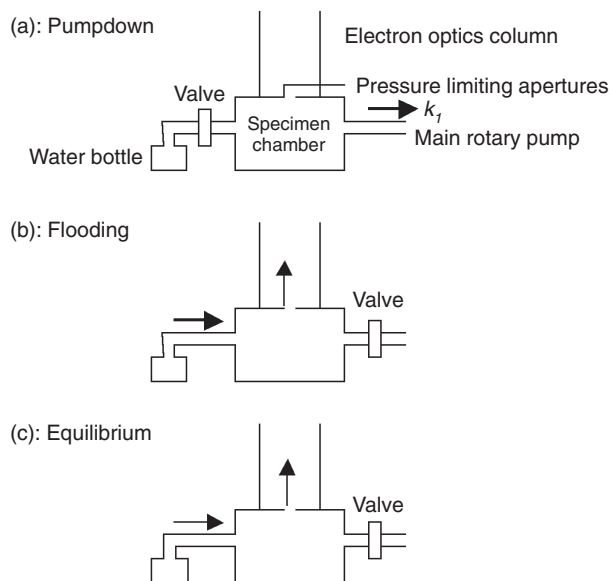


FIG. 1 The three modes of operation of the ESEM vacuum system. Pumpdown (a) is the removal of air and water vapour from the specimen chamber by the main rotary pump; flooding (b) is the injection of water vapour into the specimen chamber from the water bottle; and equilibration (c) is the residual flow of air and water vapour into the electron optics column, matched by an equal flow from the water bottle (Cameron and Donald 1994).

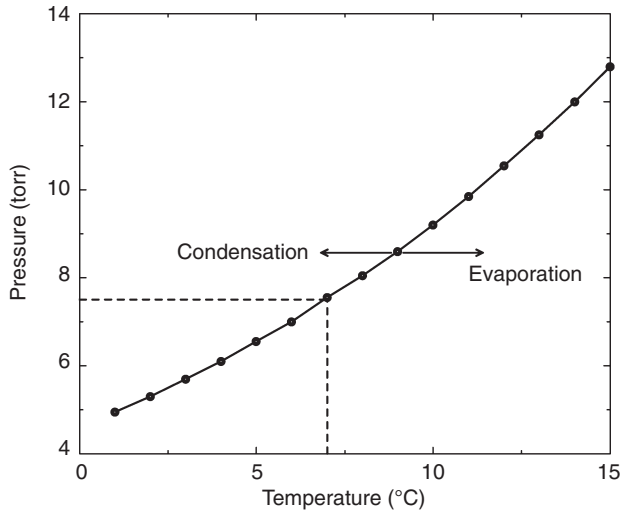


FIG. 2 The saturated vapour pressure line for water, in the ESEM pressure range. The condensing and evaporating regimes are shown. Dotted lines show the conditions used in this experiment, 7.0°C and 7.5 torr (1 atm=760 torr).

Although the specimen can be stabilised in the ESEM, the pumpdown process produces some highly unstable conditions. Initially, the specimen is placed in the ESEM and exposed to air at room temperature and a pressure of 1 atm (760 torr). This air is then pumped out of the chamber until the pressure is close to the operating pressure of a few torr and replaced by water vapour. However, during this pumpdown, the vapour pressure of water can fall to very low levels indeed, increasing the rate of evaporation enormously. If the total pressure of water vapour *and air* in the chamber falls below the SVP, then boiling will occur, which may disrupt the specimen.

Boiling is prevented by pumping down such that the total pressure (air and water vapour) does not fall below the SVP of the specimen. Successions of “floods” are then carried out, in which water vapour is introduced to the ESEM specimen chamber from a water bottle, which raises the total chamber pressure. After flooding by around 4 torr, a further pumpdown is carried out to bring the pressure back down to the saturated vapour pressure. Each successive flood-pump cycle removes air from the mixture, which is eventually almost all water vapour. Cameron and Donald (1994) showed that after nine flood cycles, the atmosphere was 99% water vapour. Note that k_1 , k_2 , and k_3 are taken from values determined by Cameron and Donald (1994) for an Electroscan E3 ESEM and are tabulated in Table I for convenience.

Now Cameron and Donald (1994) noted that considerable evaporation can occur during initial pumpdown, as the water vapour pressure can fall to very low levels indeed. However, this evaporation can be lessened by raising the water vapour pressure in the chamber by introducing a water source. A drop of water placed close to the specimen, but held at ambient temperature rather than 7.5°C, evaporated preferentially to the specimen.

TABLE I The values for the rate constants for the pumping, flooding and equilibration stages in ESEM pumpdown. These values were obtained by Cameron and Donald (1994)

k_1	0.07s ⁻¹
k_2	0.00097s ⁻¹
k_3	0.02152s ⁻¹

We now seek to incorporate this additional water source in the model of Cameron and Donald (1994). Three modes of pumpdown and subsequent operation were identified (Fig. 1):

1. Pumpdown: Air and water vapour are removed from the specimen chamber at the same rate (Fig. 1a).
2. Flooding: Water vapour at room temperature is introduced to the chamber due to the open valve to the water bottle (Fig. 1b).
3. Equilibration: Air and water vapour flow from the specimen chamber towards the higher vacuum of the electron optics column via the pressure limiting apertures. The pressure in the specimen chamber is held constant with the flow of water vapour from the water bottle to the specimen chamber. Equilibration is therefore a residual replacement of air with water vapour due to the need to maintain a pressure gradient within the ESEM (Fig. 1c).

Pumpdown has an exponential time-dependence such that

$$\frac{dP_w}{dt} = k_1 P_w \quad (1)$$

$$\frac{dP_a}{dt} = -k_1 P_a \quad (2)$$

where k_1 is the rate constant of the main pump, P_w and P_a are the pressure of air and water, respectively, and t is time. k_1 was found to be $7 \times 10^{-2} \text{s}^{-1}$ for the ElectroScan E3 ESEM (Electroscan, Boston, Mass., USA) used here (Cameron and Donald 1994).

In equilibration mode, air is gradually removed, so

$$\frac{dP_a}{dt} = -k_2 P_a \quad (3)$$

where k_2 is the rate constant for the flow of air along the pressure gradient. k_2 was found to be $9.7 \times 10^{-4} \text{s}^{-1}$ (Cameron and Donald 1994).

This is exactly balanced by introducing water vapour,

$$\frac{dP_w}{dt} = -k_2 P_a \quad (4)$$

In flood mode, the air continues to flow through the PLAs from the specimen chamber to the electron optics col-

umn, so Eq. (3) still holds. The water vapour pressure is given by

$$\frac{dP_w}{dt} = -k_2 P_w + k_3 (X(T_r) - P_w - P_a) \quad (5)$$

$k_3 (=2.152 \times 10^{-2} \text{s}^{-1})$ is the rate constant for water vapour inflow from the water source bottle, $X(T_r)$ is the saturated vapour pressure for water, at room temperature (T_r) as the bottle is not chilled (Cameron and Donald 1994).

Note that k_1 , k_2 , and k_3 are taken from values determined by Cameron and Donald (1994) for an ElectroScan E3 ESEM, which would not be identical to the ElectroScan 2010 used in this work. However, measuring these values for the ElectroScan 2010 was not considered to be appropriate or necessary: the parameters vary considerably over time, requiring measurement before each experiment, which was not practical. Furthermore, the conclusions drawn from this section are equally applicable to the ElectroScan E3 and 2010 ESEMs and are not hugely sensitive to the exact values of k_1 , k_2 , and k_3 .

Taking 298 K (25°C) as the room temperature and relative humidity of the ambient air as 50%, the pressure variation during a pumpdown can be found, as shown in Fig. 3a. It is clear from the figure that the water vapour pressure can fall to very low levels during the initial pumpdown. This is due to a constant ratio of air to water during pumpdown.

Extending the Model

So far, a brief review of the work of Cameron and Donald (1994) has been presented. This section extends their approach to include a water source in the form of a drop of water present in the specimen chamber during pumpdown. This water source is treated as a 1 cm square at 298 K (25°C) and is assumed to have evaporated totally by the end

of the first pumpdown. The rate of water evaporation is given by

$$\frac{dm_e}{dt} = \left(\frac{k_B T_r}{2\pi m} \right) \rho_w \exp\left(-\frac{\varepsilon}{k_B T_r} \right) \left[1 - \frac{P_w}{X(T_r)} \right] \quad (6)$$

where m_e is the mass lost through evaporation, m is the mass of a single water molecule, ρ_w is the density of water, ε is the latent heat of vapourisation of a single water molecule and k_B is Boltzman's constant (Cameron and Donald 1994). Using Kaye & Laby (1995), the value of $\varepsilon/k_B T_r$ was found to be approximately 3180.

Equation (6) gives the mass of water lost from the drop due to evaporation. The increase in partial pressure due to this evaporation was determined by assuming a chamber volume of $8 \times 10^{-3} \text{m}^3$. This corresponds to the ElectroScan ESEM E3. The contribution from this additional water source is clear in Fig. 3b. Although the partial pressure of water falls during the initial pumpdown, the drop is not nearly as great as that in Figure 3a without the water source. Also, rather fewer flood-pump cycles are required before the chamber atmosphere is largely water vapour in the case of Figure 3b.

It is clear that adding a water source during initial pumpdown can significantly reduce the potential for water evaporation from aqueous specimens in ESEM. Prior to pumpdown, a water drop is placed on part of the ESEM stage which remains at room temperature. The location of the water drop is assumed not to matter, because the air and water vapour are taken to be fully mixed in the specimen chamber. This follows the treatment of Cameron and Donald (1994). Although this is clearly an approximation, to incorporate a spatial dependence into the expressions for water vapour and air pressure is beyond the scope of this work. However, the drop is placed close to the specimen, as during pumpdown the water vapour pressure is expected to be highest close to the evaporating drop.

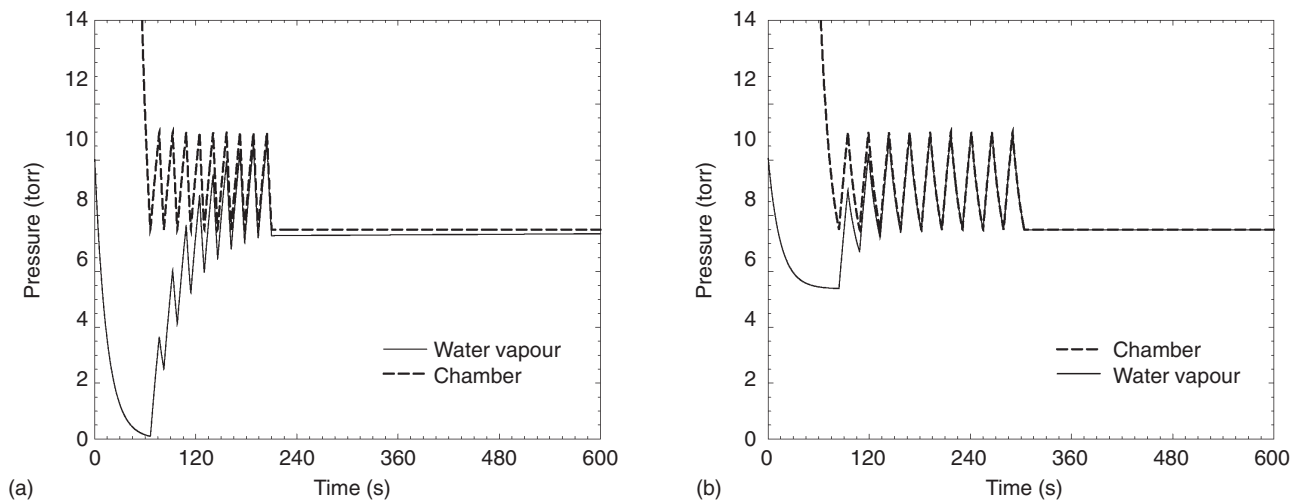


FIG. 3 Water vapour and air pressure as a function of time during the optimised pumpdown of Cameron and Donald (1994) (a), and with a water source within the specimen chamber (b).

Environmental Scanning Electron Microscope Contrast

Observed contrast in ESEM comes from two routes, backscattered and secondary electrons. Backscattered electrons are incident electrons, which have been elastically scattered strongly in the specimen so that they are ejected and thus contribute to the signal. Incident electrons interact more strongly with the larger atomic nuclei, so backscattered electrons are sensitive to atomic number (Goldstein 1992). In this case, a bright signal is associated with the relatively high atomic number of silicon in the silica particles with respect to the polymer film.

Secondary electrons are produced by ionisation events in the sample. Secondary electrons are comparatively low energy and hence have a rather small escape depth, of the order of a few nanometers. Since the penetration of incident beam electrons is much greater, the bulk of secondary electrons are produced deeper inside the specimen and reabsorbed. A sloping surface increases the chance of escape for secondary electrons at greater depths, so the signal is increased, giving rise to topographic contrast (Goldstein *et al.* 1992). Since surface roughness is related to the presence of silica at the surface (Schneider 1994), a strong secondary electron signal from regions of surface silica is expected.

A further source of secondary electron contrast is associated with the energy gap between conducting and valence electrons in the specimen (band gap). Secondary electrons can travel further before reabsorption in materials with wider energy gaps, which increases the probability of escape. The signal, therefore, is stronger from materials with wider band gaps (Stokes *et al.* 1998). For the specimens studied here, in the early stages of film formation, more water is present, which has a larger band gap than the final polymer film, and so the signal is expected to be stronger to begin with.

Materials and Methods

In this work an ElectroScan 2010 ESEM was used. The beam energy was 8 keV; this relatively low value was chosen because lower energies minimise specimen damage (Royall *et al.* 2001). Other experimental parameters were chosen to promote film formation, in particular specimen temperature and chamber pressure. The T_g of the latex used was quoted as 80°C (Allied Colloids). Although the deformation stage of film formation (stages II–III) is promoted by the addition of plasticisers, it was desirable to raise the specimen temperature as much as possible to be close to room temperature, where the latex is film forming, compared with typical ESEM specimen temperatures of 3°C (O’Dowd *et al.* 1994).

In practice, the specimen temperature chosen was limited by the chamber pressure. At pressures above 5 torr, the ESEM signal falls off (Fletcher 1997), and a chamber pressure of 7.5 torr was chosen as the highest pressure at which

the ESEM produced images of sufficient quality. Since the hydrated specimen must be kept close to saturated vapour pressure, the specimen temperature corresponding to 7.5 torr was 7.0°C. This was the highest temperature at which in situ film formation could be followed.

The specimen was chilled to 6.5°C during pumpdown to prevent any boiling. A small amount of condensation occurred as a result of this temperature suppression, which was removed by raising the specimen temperature at a rate of 0.1°C min⁻¹. The evaporation of water in this way also initiated film formation, and the temperature was increased until silica could be discerned on the surface. Film formation was then recorded in a series of image scans. This method was chosen over varying the pressure, which could equivalently have been used to initiate film formation, because temperature was easier to control precisely on the ElectroScan 2010 ESEM.

Image Analysis

The image analysis technique employed has been detailed previously (Royall 2000, Royall and Donald 2001), and is recapped here. The aim is to isolate the pixels in the ESEM image that correspond to silica. Each pixel is therefore chosen as either “silica” or “background,” according to certain criteria.

Although silica appears bright, due to small imaging instabilities in ESEM (e.g., fluctuations in electron beam intensity) simply selecting bright pixels tends not to produce reliable results (Royall 2000). Instead the change in brightness associated with silica is used to detect silica particles. The Sobel operator (S) (Russ 1995) is used to quantify the change in brightness,

$$S(I) = \sqrt{\left(\frac{\partial I}{\partial x}\right)^2 + \left(\frac{\partial I}{\partial y}\right)^2} \quad (7)$$

where $I(x,y)$ is the brightness of the pixel at (x,y) . If the Sobel operator had a value of >15, the corresponding pixel was taken to be silica. The Sobel operator tends to find the edges of the silica particles, missing a few very bright pixels in the centre. These were identified with a brightness threshold. The brightness threshold required that the pixel had a brightness value >245 on a scale from 0–255. If either or both criteria were satisfied, then the pixel was taken to be silica. By dividing the silica pixels by the total, the silica surface fraction can be obtained as a function of drying time. The gradient threshold is determined by requiring that an image with no visible silica yields only a very small fraction of pixels, around 10⁻⁵ which can be identified as silica. In this way, the noise in the system was eliminated (Royall 2000). The brightness threshold was simply chosen to be close to, but less than, 255.

Following thresholding, the image has two types of

pixel, corresponding to the silica or the polymer/water background. The silica pixels tend to be grouped in clusters, corresponding to the silica particles. These clusters can be counted and sized (Royall 2000). Thus the number of clusters can be followed during film formation. A further requirement is to ignore isolated bright pixels, which are associated with noise (Pawley 1995, Russ 1995). This is achieved by requiring that each cluster of pixels must be >10 to be treated as silica. The silica surface fraction and cluster count is then adjusted accordingly.

The image processing software used in this work was written by the authors in the C programming language and run on a unix workstation (Royall 2000).

Specimen Preparation

The details of specimen preparation have been presented elsewhere (Royall and Donald 2001). Here the main points only are noted. The lacquer was based on a polybutylmethacrylate (PBMA) latex with a diameter of 80 nm (Allied Colloids). A variety of additives were used, including a defoamer, coalescing aid, and rheology modifier. Most important, silica was incorporated at 2.5% by weight.

The silica used is a precipitated silica (Iler 1979)*. Here aggregate (1–10 μm) particles are precipitated from ultimate particles 20 nm in diameter. The aggregate particles are of interest here. For film formation, the specimen was laid out with a microapplicator on a specially made aluminium ESEM stub, as shown in Figure 4. The nominal film thickness (d_0 in Fig. 4) was 200 μm . The stub then sat in the ESEM Peltier stage and was chilled to 6.5°C prior to pumpdown.

Results and Discussion

The technique described above provided a series of images of the lacquer undergoing in situ drying, as shown in Figure 5. The images show a transition from a rather featureless aqueous dispersion to a film that may be regarded as “dry,” where silica appears bright against the polymer background. Upon removal from the ESEM, the film was indeed dry, as mentioned below.

Individual silica particles become easier to distinguish over time. For example the particle marked as (a) in Figure 5 grows brighter and larger at longer film formation times. Examination of this region shows some movement between the frames in Figure 5 taken at 15 and 59 min. This is taken to be a result of non uniform drying leading to shrinkage and/or specimen drift, which is due to relatively poor adhesion to the aluminium substrate. In Figure 5, the background becomes darker over time. This is attributed to water loss, as there should be a stronger signal from

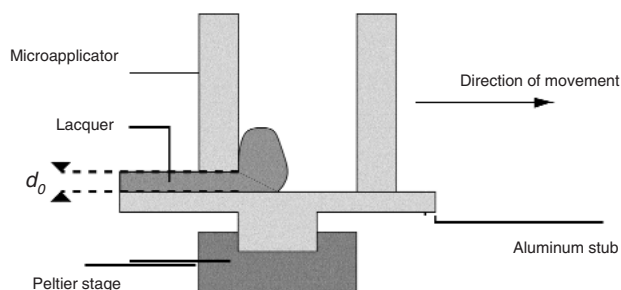


FIG. 4 Schematic experimental set-up. Movement of the microapplicator leaves a wet film of thickness d_0 (200 μm) on the substrate. The aluminum stub fits snugly in the ESEM Peltier stage.

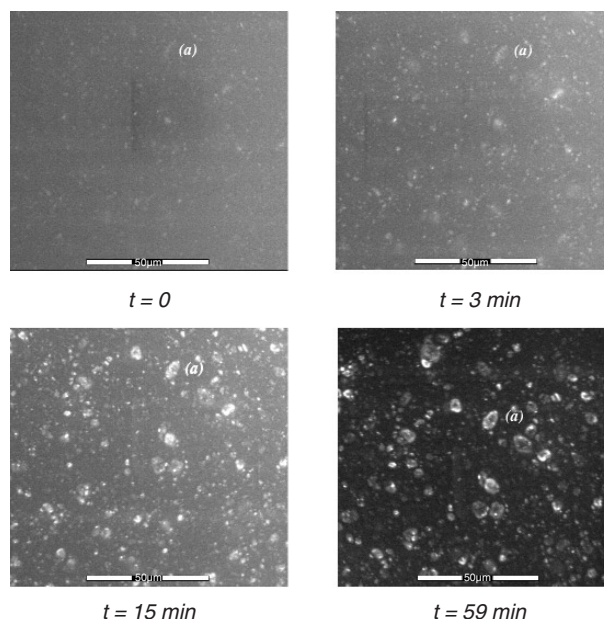


FIG. 5 Lacquer containing precipitated silica undergoing drying in the ESEM. From an aqueous dispersion, the lacquer dries to reveal silica particles. The area (a) shows how an individual particle is revealed over time. Bars=50 μm .

water, as it has a wider band gap than the polymer (Stokes *et al.* 1998). Note that the absence of visible latex particles is not surprising. At 80 nm, they are too small to show up in these images, which were produced at an original magnification of 800 \times .

A schematic of this drying process is shown in Figure 6. Here, drying is driven by volume reduction from evaporation. Initially (Fig. 6a), there is an aqueous dispersion with no structure accessible to ESEM. As water evaporates, silica begins to perturb the surface and this structure should show some contrast in ESEM (Fig. 6b).

Finally the water is removed and the film is dried, in the sense that volume reduction due to water evaporation is complete (Fig. 6c). From the ESEM images in Figure 5, this process appears to cover latex film formation in stages I–III. The lacquer produced clear films when dried at room

*Precipitated silica was supplied by Dr G. Morea-Swift at Crosfield Group, Warrington, U.K.

temperature, which is indicative of stages III–IV (Keddie 1997, O'Dowd *et al.* 1994). However, the films produced in the ESEM were white, which suggests film formation only to stage II* (Keddie 1997). It seems that the temperature suppression to 7°C meant that the latex was too rigid to deform to stage III. In other words, it behaved as a non-film-forming latex at 7°C. Nonetheless, ESEM images of film dried in situ show exactly the same features as those of films dried at room temperature, as can be seen from Figure 7. This is unsurprising, given that here we are focussing on the silica, not the latex particles. At 80 nm in diameter, the latex particles are too small to be revealed, regardless of whether or not they have deformed. Clearly a latex which is film forming at 7°C should be entirely insensitive to whether it is dried in situ or at room temperature. However, at the lengthscales used, here the technique is insensitive to whether or not the latex is film forming.

Numerical Analysis

The fraction of pixels identified as silica (silica surface fraction) is plotted in Figure 8 as a function of time. The time is taken as zero when the silica can first be seen on the surface. There is an increase in silica surface fraction with time, as would be expected from the images, except at around a time of 30 min. This drop is assumed to be due to chance specimen movement, which has already been noted from Figure 5.

The number of distinct clusters is shown as a function

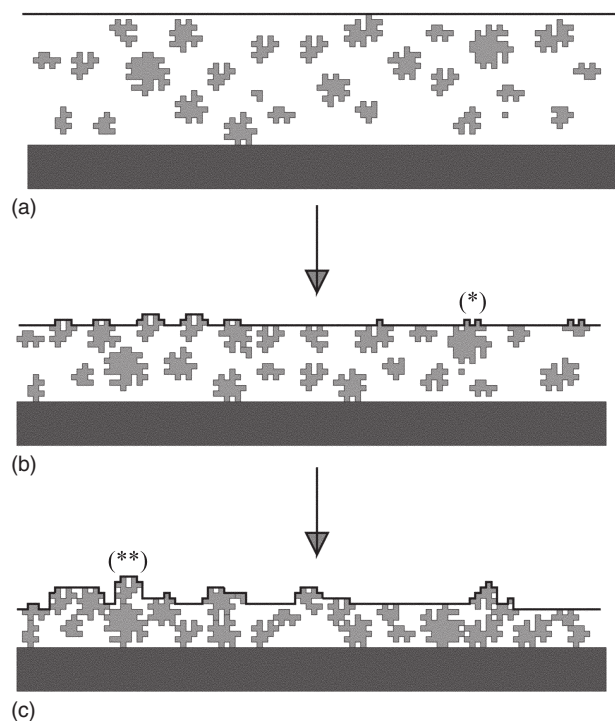


FIG. 6 Schematic of silica in aqueous lacquer during drying. Stage I of latex film formation corresponds to (a), where the silica is dispersed throughout the aqueous latex suspension; (b) and (c) are the results of stage II and III (or II*) of latex film formation, respectively.

of time in Figure 9. Like the silica surface fraction, the cluster count increases with time, although the count increases rather more quickly than the surface fraction. In other words, the silica particles are identified on the surface quite early, after around 5 min. Further drying reveals more of these same silica particles, so although the number of clusters is roughly constant, the silica surface fraction increases for drying times of up to 20 min as more of the same particles are revealed.

Although it is roughly constant, the cluster count fluctuates and is highest at around 12 min. This is taken to be due to the difference between silica particles and clusters. A cluster is a group of neighbouring white pixels, whereas a silica particle is a real object. Each silica particle can produce more than one cluster, especially at short drying times, as might be expected from the region marked (*) in Figure 6b. Alternatively, at longer drying times, several silica particles form only one cluster, such as that marked as

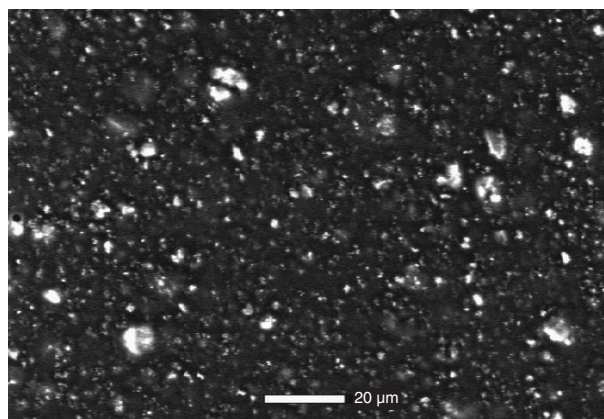


FIG. 7 Environmental scanning electron microscope image of film dried at room temperature. Exactly the same structure is shown as that for a specimen dried in situ.

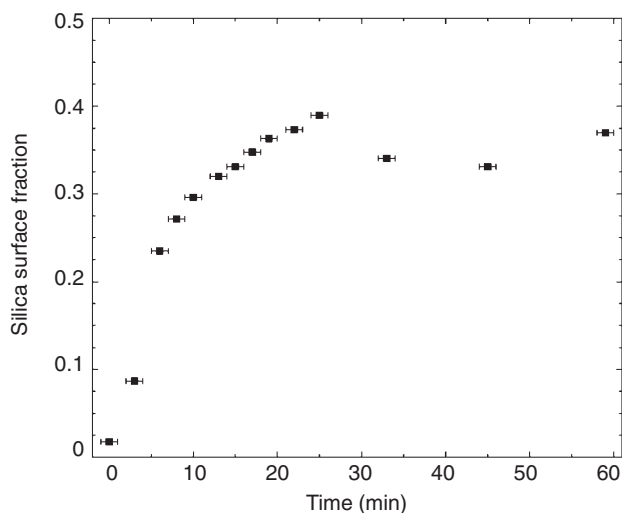


FIG. 8 Silica surface fraction as a function of drying time, which is taken from the first appearance of silica in the ESEM images.

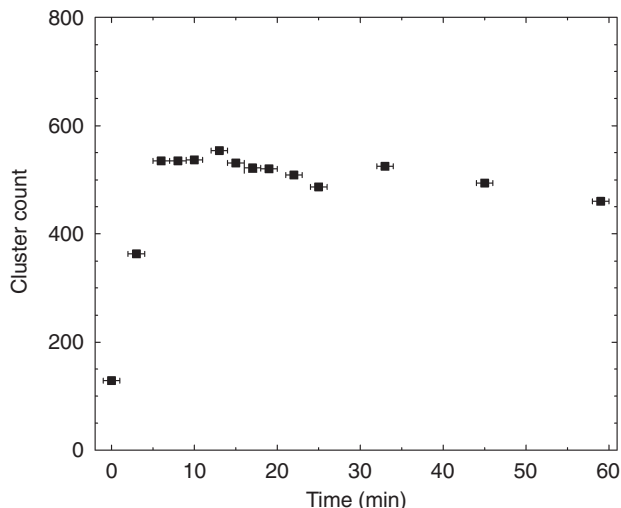


FIG. 9 Cluster count as a function of drying time.

(**) in Figure 6c.

The numerical results support the mechanism illustrated in Figure 6. The silica particles are viewed as embedded in a polymer/water matrix. Initially (Fig. 6a), silica is beneath the surface, presumably held by surface tension of the aqueous phase. Evaporation will tend to bring the surface of the increasingly concentrated dispersion down. During this period, there is competition between surface tension (which tends to keep silica below the surface) and the material below the top layer of silica particles, which tends to resist further compression.

By the time stage II of latex film formation is reached, the lower material resists compression sufficiently that the silica particles break through the water/latex surface and silica is visible on the surface (Fig. 6b). Further evaporation results in a receding surface. However the silica particles are now held up by the material below them. As the surface recedes, more and more of this top layer is exposed, so the particles appear larger and more distinct (Fig. 6c).

Conclusions

Environmental scanning electron microscopy has been shown to be a suitable tool for imaging in situ drying of matt water-based lacquers. The addition of a water source during the pumpdown stage of ESEM has been shown to be very useful in limiting specimen evaporation. Furthermore, analysis of the same region during drying has been made possible by the inclusion of silica. The contribution of the silica is twofold: It provides stronger contrast than the latex alone, and its lengthscale is such that lower magnification may be used, which reduces radiation damage, allowing drying of one region to be followed.

The volume reduction resulting from evaporation drives the transition from an aqueous dispersion, with little contrast in ESEM, to a polymer film with silica particles present on the surface. The transition appears to be gradual,

with continuous water loss. Peaks of particles are seen first, before the remainder is revealed by further volume loss from water evaporation.

One possible improvement to the pumpdown process would be partially to open the valve to the ESEM water bottle during initial pumpdown. With monitoring of the k_{1-3} parameters and careful control of the water inflow, it should be possible to maintain saturated vapour pressure throughout pumpdown, which would eliminate specimen condensation and evaporation during pumpdown.

This technique could be applied to other systems: any latex with hard inclusions should be accessible to this methodology. In particular, the silica could be substituted with pigment for analysis of pigmented lacquers. Other systems that could be studied include sunscreen (where the titanium dioxide screening agent would provide considerable atomic number contrast), lipstick, and other cosmetics. However, the effects of temperature suppression to around 7°C should not be overlooked. This tends to inhibit film formation, such that a film-forming latex at room temperature may not proceed beyond stage II* at 7°C, as is the case in this work. However, the features of interest are not strongly sensitive to latex deformation, so the lack of latex deformation has little effect on the images recorded.

Environmental scanning electron microscopy is not limited to water-based systems. Oil-based systems can also be imaged (Stokes *et al.* 1998). Here, the technique is rather simpler; due to their typically low vapour pressure, oil-based specimens are stable in the ESEM, so there is no need to maintain the saturated water vapour pressure in the specimen chamber. Oil-based lacquers can therefore be imaged at room temperature. Like water-based systems, some form of hard inclusion would be desirable to promote contrast.

Acknowledgments

The authors would like to thank the Engineering and Physical Sciences Research Council and Crosfield Group for funding, and in particular Drs G. Morea-Swift of Crosfields, B.L. Thiel for ESEM pumpdown help, and Drs. G. Soga and O.M. Astley for discussions relating to image analysis.

References

- Allied Colloids, Coatings and Specialities Division, Allied Colloids Ltd, Bradford, West Yorkshire, UK. *Glascal C47, technical and processing data*
- Brown GL: Formation of films from polymer dispersions. *J Polymer Sci*, 12, 423–434 (1956)
- Cameron RE, Donald AM: Minimizing sample evaporation in the environmental scanning electron microscope. *J Microsc*, 173, 227–237 (1994)
- Danilatos G: Introduction to the ESEM instrument. *Microsc Res Tech* 25, 354–361 (1993)

- Gate L, Windle W, Hine M: The relationship between gloss and surface microtexture of coatings. *Tappi* 56, 3, 61–65 (1973)
- Fletcher AL: *Cryogenic Developments and Signal Development and Environmental Scanning Electron Microscopy*, PhD Thesis. University of Cambridge, U.K. (1997)
- Goldstein JI: *Scanning Electron Microscopy and X-ray Microanalysis*, 2nd Ed. Plenum Press, New York (1992)
- Iler RK: *The Chemistry of Silica*. John Wiley & Sons, New York (1979)
- Kaye GWC, Laby TH: *Tables of Physical and Chemical Constants*, 16th Ed. Longman, Harlow, England (1995)
- Keddie JL, Meredith P, Jones RAL, Donald AM: Rate-limiting steps in film formation as elucidated with ellipsometry and environmental scanning electron microscopy. *ACS Symposium Series*, 648, 332–348 (1996)
- Keddie JL: Film formation of latex. *Mater Sci Engineer R*, 21, 101–170 (1997)
- O'Dowd ML, Sperry PR, Snyder BS, Lesko PM: Role of particle deformation and compaction in latex film formation. *Langmuir*, 10, 2619–2628 (1994)
- Pawley JB: *Handbook of biological confocal microscopy*, 2nd Ed. Plenum Press, New York (1995)
- Royall CP: The behaviour of silica in matt water based lacquer, PhD Thesis, University of Cambridge, U.K. (2000)
- Royall CP, Donald AM: Confocal microscopy and environmental SEM applied to matting water-based lacquers (Eds. Provder T, Urban MW). Film formation in coatings, *ACS Symposium Series* 790, 193–211 (2001)
- Royall CP, Thiel BL, Donald AM: Radiation damage of water in environmental scanning electron microscopy, *J Microsc*, 204, 185–195 (2001)
- Russ JC: *The Image Processing Handbook*, 2nd Ed. CRC Press, Boca Raton, USA (1995)
- Schneider H: Matting of modern surface coatings. *Surf Coat Intl* 77, 376–385 (1994)
- Stokes DJ, Thiel BL, Donald AM: Direct observation of water-oil emulsion systems by environmental scanning electron microscopy. *Langmuir* 14, 4402–4408 (1998)
- Talmon Y: Electron beam damage to organic and biological cryospecimens. In *Cryotechniques in Biological Electron Microscopy* (Eds. Stinbrecht RA, Zierold K), Springer-Verlag, Berlin (1987) 64–84